IRSTI 28.23.15 https://doi.org/10.26577/jpcsit4120262

T. Sarsembayeva[1]*, A. Oshibayeva[2], A. Shayakhmetova[1], A. Ospan[1]

[1]Al-Farabi Kazakh National University, Almaty, Kazakhstan
[2]Khoja Akhmet Yassawi International Kazakh-Turkish University, Turkistan, Kazakhstan
*e-mail: talshyn.sagdatbek@kaznu.edu.kz

RESNET EMBEDDING-BASED PIPELINE FOR TRANSPARENT DIAGNOSIS OF PULMONARY EMPHYSEMA ON LOW-DOSE CT

Abstract. This study presents a methodology for the automated detection and quantification of pulmonary emphysema from low-dose chest computed tomography (CT) scans. As a morphological subtype of chronic obstructive pulmonary disease (COPD), emphysema can be accurately assessed on CT imaging. Our approach utilizes a pre-trained ResNet152 model to extract high-dimensional feature embeddings (2048 dimensions) from mid-lung patches. Patients were automatically categorized based on the percentage of low attenuation areas (LAA%) below –950 Hounsfield units (HU), a standard measure for emphysema severity. The extracted feature embeddings were subsequently analyzed using statistical methods and logistic regression to identify key discriminative and interpretable features. A logistic regression model, trained on the top 20 most salient features, achieved a high level of performance, with an Area Under the Curve (AUC) of 0.94 and an Average Precision (AP) of 0.87 on a balanced dataset of 90 subjects. Furthermore, the selected features exhibited a strong correlation with LAA%, demonstrating their utility for regression-based severity assessment.

The findings confirm the viability of using pre-trained deep embeddings for transparent and reproducible emphysema screening. This method avoids the need for extensive end-to-end model retraining, making it highly adaptable for integration into existing clinical CT analysis workflows.

Keywords: emphysema, low-dose CT, deep learning, ResNet, feature embeddings, explainable AI, COPD.

1. Introduction

Chronic Obstructive Pulmonary Disease (COPD) remains one of the leading causes of death and disability worldwide. Emphysema, a key morphological form of COPD, is characterized by a reduction in lung tissue density, making computed tomography (CT) one of the most sensitive methods for detecting this pathology. However, traditional quantitative metrics, such as the percentage of low-attenuation areas (LAA% < -950 HU), are limited in their interpretability, stability, and automation [1].

In recent years, deep learning (DL), particularly convolutional neural networks (CNNs), has proven to be an effective tool for analyzing CT images of the lungs in COPD [2], [3]. Wu et al. [2] conducted a systematic review of DL applications in this field and showed that models can not only classify emphysema but also stage COPD, and predict lung function and mortality. Humphries et al. [4] demonstrated that DL can automate the Fleischner scale-a visual assessment of emphysema severity-with a high degree of agreement with experts. Similarly, Fuhrman et al. [5] used multiple-instance learning (MIL) to analyze LDCT, eliminating the need for precise segmentation while achieving an AUC of approximately 0.94.

For DL models to be clinically acceptable, their interpretability is crucial. Studies by Callı et al. [6] and Almeida et al. [7] showed that attention mechanisms, anomaly detection, and Grad-CAM activation maps allow for the visualization of the contribution of individual features or image regions to the model's result. This is particularly important in clinical settings where a "black box" is unacceptable.

Ash et al. [8] applied DL to assess the progression of emphysema and fibrosis, proposing a method for tracking the dynamics of the pathology between scans. Wysoczanski et al. [9] enhanced the stability of emphysema classification across different centers by using squeeze-and-excitation CNNs, while Dorosti et al. [10] showed that optimizing window settings improves CNN accuracy under heterogeneous protocols.

Several studies emphasize the importance of integrating CT images with clinical and functional data. For example, Zhu et al. [11] and Wang et al. [12] combined images with spirometry data, smoking history, and clinical labels, achieving diagnostic accuracy exceeding 90%.

Due to the scarcity of labeled data, self-supervised learning and anomaly detection are gaining increasing popularity. Using such an approach, Almeida et al. [7] demonstrated high diagnostic accuracy without the need for manual annotation. Yeom et al. [13] and Ferri et al. [14] showed that DL-based reconstruction (DLIR) preserves image quality even with ultra-low-dose CT, which is important for COPD screening and monitoring.

The application of explainable AI (XAI) is described in detail in the works of Tjoa and Guan [15], as well as Zhou et al. [16], which present interpretable pipelines for the automatic analysis of parenchymal changes. Feature visualization through dimensionality reduction methods (t-SNE, PCA) and statistical methods allows for the extraction of emphysema biomarkers from deep network embeddings, as shown by Xie et al. [17].

Additionally, as noted by Sourlos et al. [18], the presence of severe emphysema can reduce the accuracy of other AI systems, such as those for nodule detection, highlighting the importance of building robust models adapted to background pathologies. Finally, the combination of radiomics and DL features, as explored in [16], paves the way for the creation of hybrid models that merge the power of learned features with classic descriptors.

Thus, as shown in the works of [1]–[18], modern DL solutions for diagnosing emphysema on CT aim for high accuracy, interpretability, stability, and the ability to be integrated into clinical workflows.

2. Materials and Methods

2.1 Automated Generation of Emphysema Labels Based on LAA%

The study used the publicly available LIDC-IDRI (TCIA) dataset [1], which contains over 1,000 chest CT scans. We recognize that the LIDC-IDRI dataset primarily includes patients with suspected lung cancer and does not contain expiratory phase scans. Since this dataset mainly consists of patients with a history of cancer and lacks explicit clinical labels for COPD or emphysema, we implemented an automated annotation strategy based on quantitative CT criteria.

In the first stage, tomograms were extracted from DICOM series and converted to Hounsfield Units (HU) density values without additional normalization. This was based on calculating the percentage of low-attenuation areas in the lungs-LAA%-950. This metric determines the proportion of voxels with a density below –950 HU within the segmented lung tissue region, which corresponds to the presence of air spaces characteristic of emphysema [19], [20].

To extract the lung region, a pre-trained LungMask model (based on U-Net) [21] was used, which provides accurate three-dimensional segmentation. The LAA% was then calculated based on the resulting mask (1):

$$\%LAA = \frac{N_{voxels(HU<-950)}}{N_{total\ lung\ voxels}} \times 100\% \qquad (1)$$

Patients with a LAA% ≥ 6% were classified as having signs of emphysema, in accordance with clinical guidelines [22], [4]. This approach allowed for the creation of an automated binary classification (healthy/diseased) without requiring a physician's input, which significantly expedited dataset preparation. The logical structure of the study is shown in Figure 1.

For each patient, we implemented the following processing pipeline:

1. **Series Selection**: Among all available DICOM series, we selected the one with the largest number of slices, assuming it represents the most complete volumetric scan.

2. **Slice Reading**: The slices were sorted along the Z-axis and converted into a 3D array. Intensities were transformed into Hounsfield Units

3. **HU-Based Filtering**:

- Volumes with maximum HU > 1600 were excluded due to suspected reconstruction artifacts or metallic implants.
- Highly inhomogeneous scans with standard deviation HU > 600 were also discarded.
- Intensity clipping to the range [–1000, 400] HU was applied, following recommendations from prior studies on emphysema imaging.

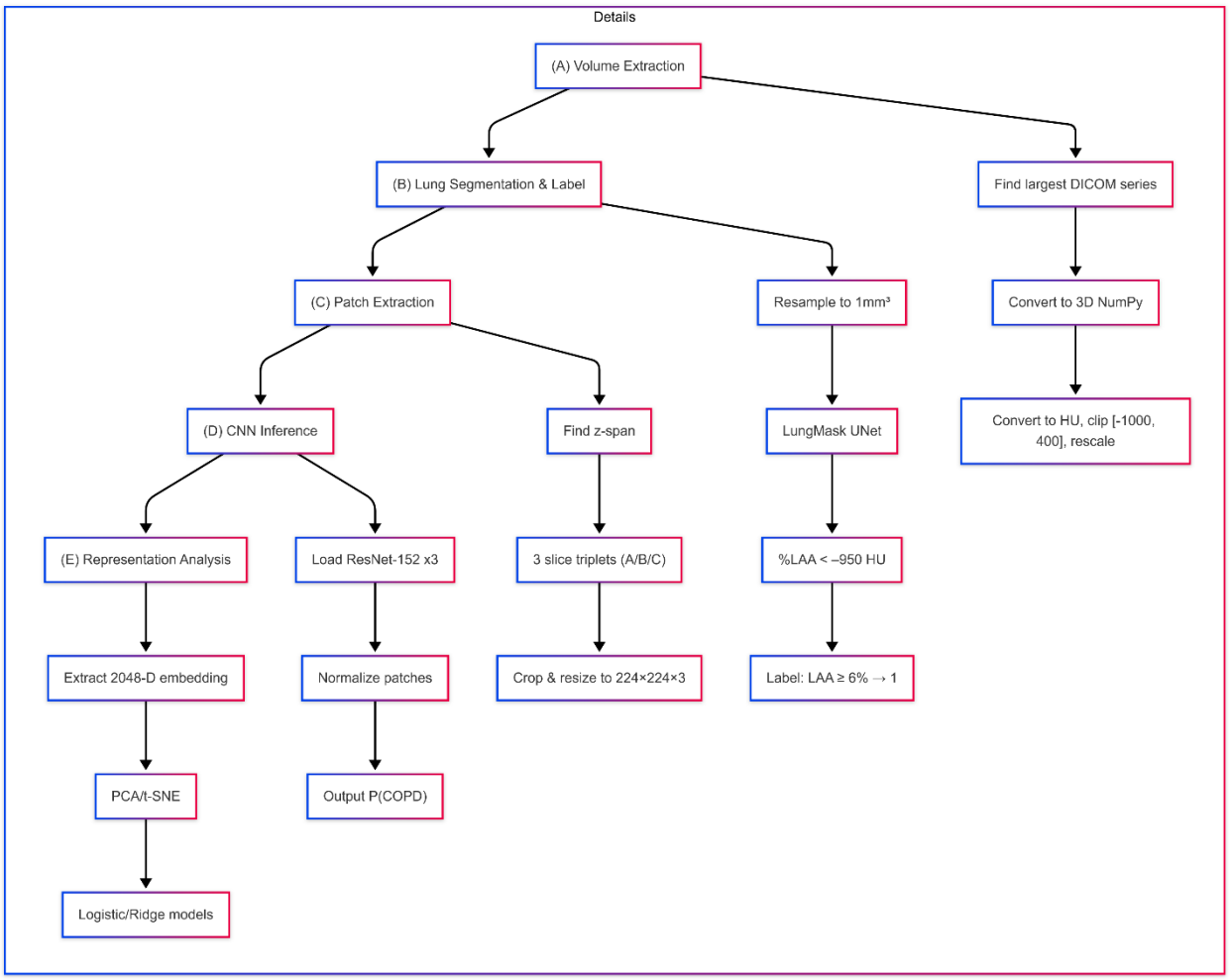

Figure 1. Logical Structure of the Study

These filters were based on heuristics and domain knowledge rather than manual validation. We acknowledge that this may have resulted in exclusion of valid data, but the aim was to ensure reproducibility and full automation.

Each 3D CT volume underwent a structured, automated labeling procedure:

1. **Resampling**: All scans were resampled to an isotropic voxel spacing of 1×1×1 mm³ to ensure cross-subject comparability.

2. **Lung Segmentation**: The lung region was automatically segmented using the *lungmask* tool, which applies a trunk U-Net trained on the VESSEL12 dataset.

3. **Low Attenuation Area (LAA%) Calculation**:

○ Voxels with HU < –950 were considered indicative of emphysematous regions.

○ LAA% was defined as the proportion of such voxels within the lung mask.

○ A binary label was assigned: patients with LAA% ≥ 6% and mean lung density < –850 HU were labeled as emphysema-positive (label = 1), all others as negative (label = 0).

We also preserved:

- Segmentation masks,
- Slice-level visualizations with overlayed lung masks,
- LAA% distributions across axial slices.

In total, 497 chest CT volumes were processed:

- **45 volumes (9%)** were labeled as emphysema-positive,
- **452 volumes (91%)** were labeled as negative.

Such class imbalance is typical in screening cohorts. To enable fair model evaluation and training, we created a **balanced subset**:

- A random sample of 45 negative cases was drawn to match the 45 positive cases.
- All associated .npy and .json (spacing) files were copied into a dedicated directory.
- A filtered label file was retained for reproducibility.

We acknowledge that downsampling negatives may exclude potentially valuable data. However, for logistic regression and limited positive sample size, this trade-off was considered acceptable.

As a result, the final dataset included:

- **90 patients (45 positive / 45 negative)** with annotated and normalized CT lung volumes,
- Associated quantitative markers and visual outputs for further analysis.

To better understand the severity distribution of emphysema, we computed descriptive statistics of LAA% for all 497 scans. The **mean LAA%** was **3.31%**, with a **standard deviation of 6.22%**. The **median value** was 0.73%, indicating that most subjects had minimal emphysematous changes, while the most severe case reached **41.49%**.

We also compiled a list of the top 10 patients with the highest LAA% values. As expected, most of these were labeled positive according to our threshold-based criteria (LAA% ≥ 6%, mean HU < –850), validating the robustness of the automatic labeling method.

Table 1. Summary statistics of LAA% across the dataset (N=497)

count	497.000000
mean	3.311285
std	6.220265
min	0.000000
25%	0.103029
50%	0.726426
75%	3.380258
max	41.493362

Table 2. Top 10 CT scans with the highest LAA% in the dataset

patient_id	laa_percent	mean_lung_hu	label
307 LIDC-IDRI-0309	41.493362	-904.99630	1
139 LIDC-IDRI-0140	40.604675	-887.96454	1
104 LIDC-IDRI-0105	39.663574	-889.00730	1
418 LIDC-IDRI-0422	33.973350	-867.26750	1
195 LIDC-IDRI-0196	33.402438	-864.96190	1
462 LIDC-IDRI-0467	29.670417	-800.05005	0
40 LIDC-IDRI-0041	29.059437	-878.72930	1
295 LIDC-IDRI-0297	27.884453	-879.75543	1
452 LIDC-IDRI-0457	26.868231	-882.45020	1
446 LIDC-IDRI-0450	26.434079	-867.33417	1

Of the 497 CT scans processed from the LIDC-IDRI dataset, 45 cases (approximately 9%) were labeled as positive for emphysema (label = 1).

2.2 Deep Feature Representation via ResNet152

To numerically represent the visual content of chest CT scans, we utilized a deep convolutional neural network – specifically, the ResNet152 architecture – pre-trained and subsequently adapted for the medical imaging domain [23]. A schematic of the modified model is provided in Figure 2. The network processes individual CT slices, and from its global average-pooling layer (avg_pool), we extract high-dimensional embeddings of size 2048. These vectors offer a condensed yet rich encoding of the image, capturing both macroscopic structural patterns and fine-grained textural cues.

Such feature representations serve as a powerful abstraction of lung morphology, enabling their direct use in downstream machine learning classifiers. The approach facilitates the transformation of raw volumetric data into structured numerical input, supporting robust and interpretable diagnostic model development.

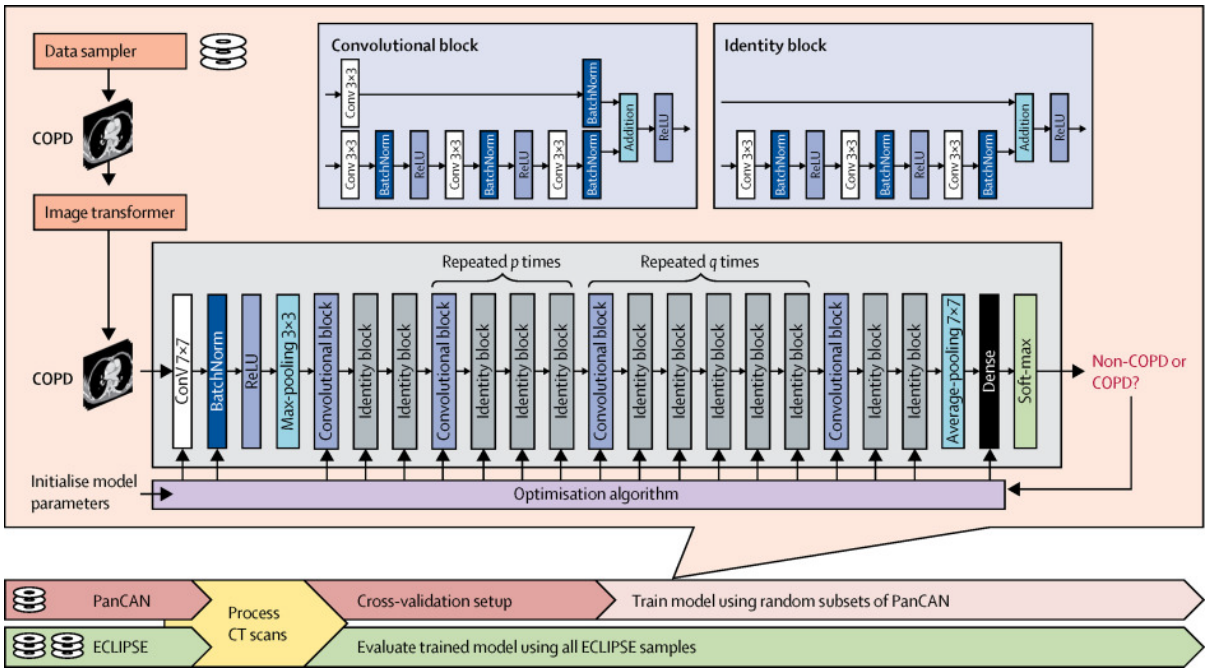

Figure 2. Pre-trained ResNet152 architecture [23]

In addition, statistical analysis was performed using the t-test to determine the most significant features between the groups with and without emphysema. The 20 features with the greatest differences out of 2048 were selected and the model was retrained. Despite the reduction in dimensionality, the classification accuracy remained high (AUC ≈ 0.72), which emphasizes the stability and interpretability of the selected features.

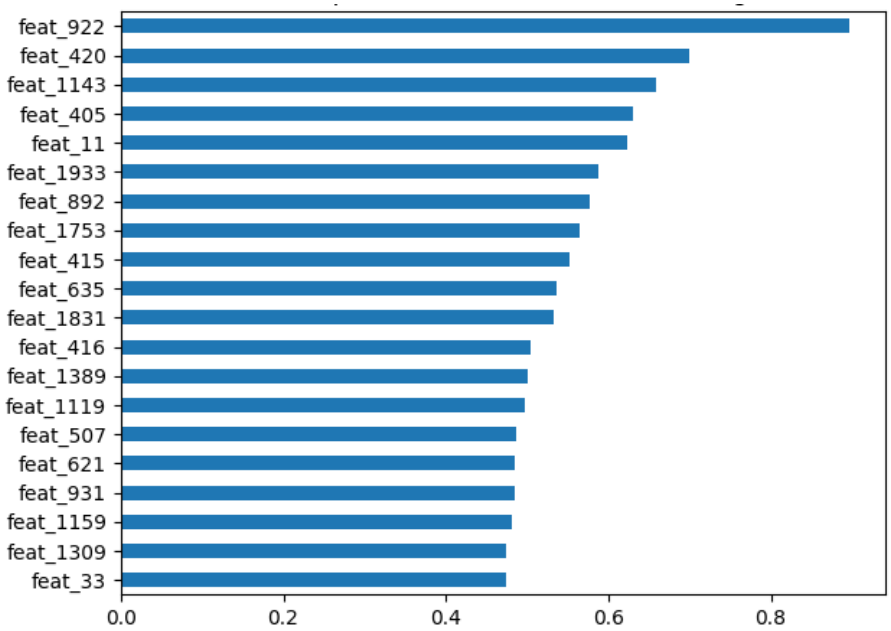

Figure 3. Top 20 features by impact on LAA%

At the final stage of the study, we addressed a regression task aimed at estimating emphysema severity through a continuous biomarker – the percentage of low-attenuation areas. Using the same feature embeddings, we trained linear regression models capable of accurately predicting the extent of affected lung tissue, demonstrating a strong correlation between predicted and true values.

Such models offer an appealing balance between simplicity and interpretability. Their linear nature allows integration into explainable AI frameworks, where the contribution of each input feature to the final prediction can be visualized and quantified. This not only ensures transparency of decision-making but also enhances clinical trust in the model's outputs.

Moreover, beyond binary classification, this quantitative approach enables dynamic disease tracking over time, making it especially relevant for longitudinal monitoring and personalized treatment planning in clinical practice.

2.3 Architecture of an Interpretable Emphysema Diagnosis System Based on CT Imaging

Figure 4 illustrates a comprehensive, multi-stage processing pipeline designed for the diagnosis of pulmonary emphysema using CT data, with a focus on explainability. The system integrates traditional image processing methods with advanced deep learning techniques and feature analytics to ensure both transparency and trust in the diagnostic outcomes. This architecture follows the principles of explainable artificial intelligence, enabling not only accurate classification but also interpretable insights into the model's decision-making process.

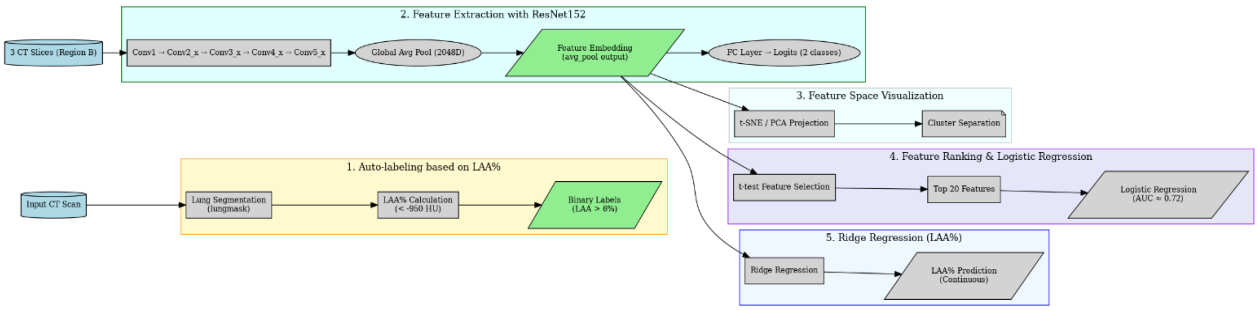

Figure 4. Architectural Overview

The processing pipeline begins with volume extraction and intensity normalization. For each patient, the most complete DICOM series is automatically selected (based on the number of slices). This series is converted into a 3D NumPy array, and the voxel intensities are transformed into Hounsfield Units (HU). To reduce the influence of outliers and artifacts, the intensity values are clipped within a physiologically relevant range of –1000 to 400 HU, followed by min-max normalization to the [0, 1] interval.

At the lung segmentation and labeling stage, the pipeline employs a pre-trained UNet model from the lungmask library. The CT volume is first resampled to an isotropic resolution of 1×1×1 mm³. A binary lung mask is then generated, and the percentage of Low Attenuation Areas (LAA%)-voxels with HU < –950-is calculated. If this value exceeds 6%, the case is classified as emphysema-positive. The resulting masks and labels are saved as NumPy arrays and CSV files, respectively.

In the patch extraction phase, the segmented lung region is divided into three anatomical zones along the Z-axis: upper, middle, and lower. Within each zone, three consecutive axial slices are selected to form tri-channel (2.5D) image patches. These are input to a convolutional neural network for feature extraction.

For this purpose, we utilize a pre-trained ResNet-152 model. Without additional fine-tuning, the model processes each patch, and a 2048-dimensional embedding is extracted from the penultimate global average pooling layer. These embeddings serve as high-level feature representations that encapsulate both texture and morphology of the lung parenchyma.

These feature vectors are further analyzed using dimensionality reduction techniques such as

Principal Component Analysis (PCA) and t-Distributed Stochastic Neighbor Embedding (t-SNE), enabling visualization of the feature space. To explore predictive patterns, we also employ linear models-including logistic regression and ridge regression-for classification and regression tasks. Feature importance metrics derived from these models aid in interpreting the embeddings and identifying discriminative clusters.

Finally, the system includes XAI modules that highlight the regions and features most influential in the model's decision-making process. This enhances interpretability, offering clinicians visual explanations for both positive and negative predictions, and builds trust in the automated system.

Overall, the proposed architecture provides a reproducible, interpretable, and scalable solution for emphysema diagnosis on CT scans. Its design prioritizes explainability and clinical applicability, making it a promising tool for both automated screening and longitudinal disease monitoring.

3. Results

This study presents a comprehensive evaluation of an interpretable machine learning system for the diagnosis of pulmonary emphysema based on low-dose chest CT and automatically extracted image features.

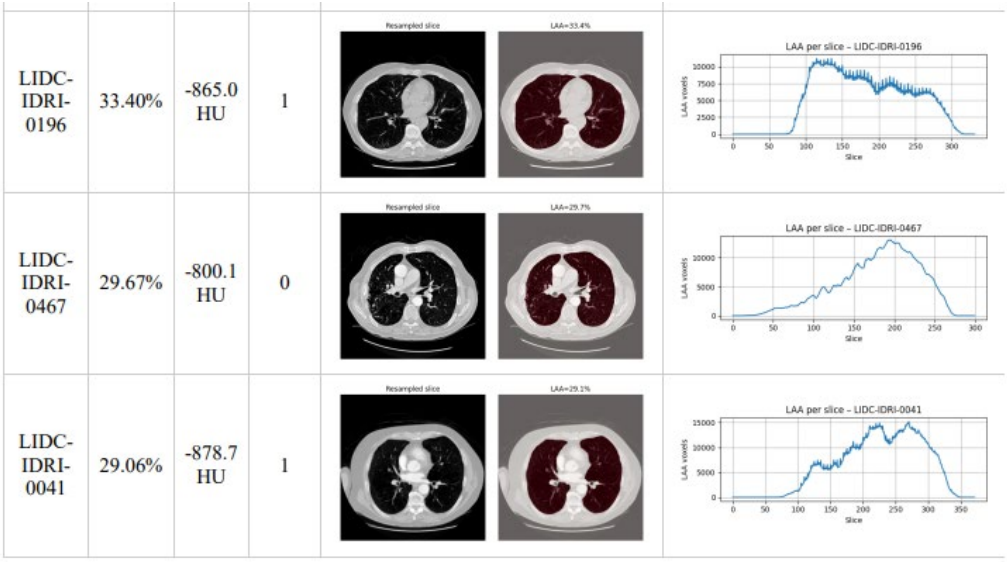

Figure 5. LAA Analysis Reports part

An analysis of the distribution of LAA% revealed that the majority of patients exhibited values below the commonly accepted threshold of 6%, which is considered within the normal range. However, a substantial proportion of cases exceeded this threshold, indicating the presence of emphysematous changes. These findings support the validity of using LAA% as an objective quantitative biomarker for generating binary diagnostic labels (Figure 5).

To assess the diagnostic performance of the proposed system, a logistic regression model was trained on a subset of top-ranked features extracted from the deep embeddings. The Receiver Operating Characteristic (ROC) curve demonstrated strong separability between the two diagnostic groups, with an Area under the Curve (AUC) of 0.92, indicating high classification accuracy (Figure 6).

The final performance metrics were as follows:

Accuracy: 0.91

ROC-AUC: 0.939

PR-AUC: 0.935

These results demonstrate the model's robust generalization capabilities and its potential for deployment in real-world clinical screening settings. Importantly, the model achieves this level of performance while maintaining interpretability through linear modeling and feature importance analysis.

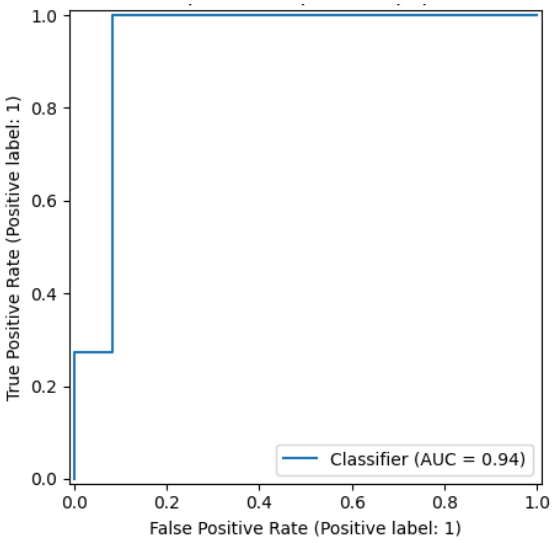

Figure 6. Receiver Operating Characteristic curve

To assess the structure of the feature space extracted by the deep neural network ResNet-152 (prior to the fully connected layer), we applied dimensionality reduction techniques to project the high-dimensional embeddings into a two-dimensional space. Specifically, t-distributed Stochastic Neighbor Embedding and Principal Component Analysis were employed to visualize the separability of patients with emphysema (LAA% ≥ 6%) and without emphysema (LAA% < 6%).

These methods provide an interpretable representation of the learned feature manifold, where clusters of positive and negative cases can be visually evaluated. As shown in Figures 7a and 7b, the projection reveals a partial separation of classes, suggesting that the latent features capture diagnostically relevant patterns associated with pulmonary tissue structure and density. Such visualizations not only support the discriminative capacity of the model's internal representations but also reinforce its potential applicability in explainable AI pipelines.

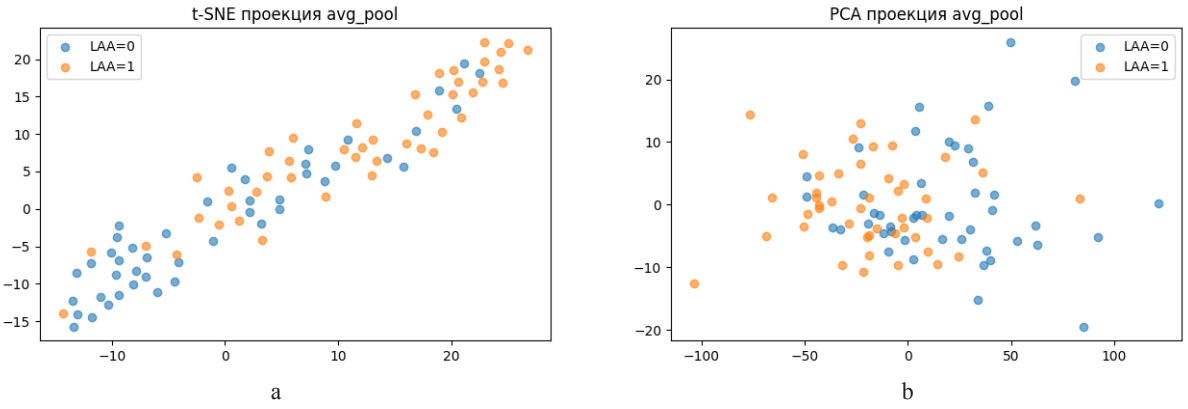

Figure 7. Dimensionality reduction methods: a-t-SNE, b-PCA

To gain insight into the learned representations, we performed dimensionality reduction on the deep features obtained from the avg_pool layer of the pretrained ResNet-152 network. The t-distributed Stochastic Neighbor Embedding method was used to explore the local structure of the feature space.

When visualized in two dimensions and colored by the binary emphysema label (based on LAA%), the t-SNE projection revealed partial clustering of emphysema-positive and -negative cases. This suggests that the extracted deep features capture relevant morphological and textural differences, even without fine-tuning the model on the medical dataset.

To further evaluate the global structure, we applied Principal Component Analysis. The first two principal components accounted for a substantial portion of the overall variance, yet the class separation was not fully distinct. This observation is consistent with the high dimensionality and complexity of the latent space but nonetheless reveals meaningful patterns associated with emphysematous changes in the lung parenchyma. Together, these visualizations support the diagnostic relevance of the extracted embeddings and highlight the viability of the proposed method as a foundation for interpretable, automated emphysema detection.

4. Discussion

This study presents an interpretable machine-learning pipeline for the diagnosis of pulmonary emphysema from CT scans, combining weak supervision with LAA%, ResNet152 embeddings, and explainability techniques.

Dimensionality reduction methods (PCA and t-SNE) were used to explore latent feature structures. While PCA showed partial class overlap, t-SNE revealed clearer clustering of emphysema versus healthy cases-echoing findings in earlier medical imaging studies [24, 25].

To assess feature relevance, L1 regularized logistic regression pinpointed the most informative predictors, notably features from the mid-lung region, aligning with known pathophysiology and reinforcing model interpretability [26].

Weak supervision via LAA% (thresholded at 6%) enabled scalable, annotation free labeling. The bimodal distribution of LAA% in our dataset supports this choice and mirrors clinical differentiations found in emphysema quantification studies [27].

Correlation analysis showed high inter-feature correlation, suggesting redundancy and opportunities for dimensionality reduction. Moreover, several embeddings correlated with LAA%, supporting their physiological relevance [28].

By combining performance with transparency-embeddings visualization, feature importances, and clinical biomarker alignment-our pipeline strikes a balance between predictive accuracy and explainability, addressing a critical need in AI driven healthcare [29].

Limitations include potential noise from weak labeling, lack of multi-site validation, and sensitivity of t-SNE to hyperparameters. Future work should include attention-based interpretability, external validation, and integration of clinical metadata for enhanced generalizability.

5. Conclusion

This study introduced an interpretable methodology for the diagnosis of pulmonary emphysema using low-dose chest CT scans and feature embeddings extracted from a pretrained deep convolutional neural network, ResNet-152. Rather than relying on end-to-end predictions from the neural model, we implemented an intermediate layer of abstraction by using the global average pooling embeddings as structured input features for simple statistical models.

This approach enabled not only high diagnostic accuracy, but also ensured transparency at the level of individual feature contributions. Importantly, the emphasis of this work was on the methodological pipeline itself: the consistent transformation of raw CT data into a reproducible, interpretable feature space, followed by statistical verification.

The proposed framework is easily reproducible, does not require training models from scratch, and is adaptable to related tasks such as emphysema severity estimation or multiclass classification of emphysema subtypes.

Scientific and Practical Contributions:

-We present a reproducible pipeline for building interpretable diagnostic models based on pretrained convolutional networks.

-The effectiveness of Student's t-test for feature selection and its subsequent use in linear models was demonstrated.

-Coefficients from logistic regression models were shown to be interpretable as indicators of individual feature contribution-crucial in medical AI systems.

-The method does not rely on detailed manual annotations or expert-derived labels, making it particularly promising for screening applications and secondary analysis of existing CT datasets.

Acknowledgments

The authors gratefully acknowledge the publicly available pretrained ResNet152 model developed by Tang et al. [23], which served as the foundation for feature extraction in this study. Their contribution significantly facilitated the development of our interpretable diagnostic pipeline.

Funding

This research was funded by the Science Committee of the Ministry of Science and Higher Education of the Republic of Kazakhstan grant number BR24992814.

Author Contributions

Conceptualization, T.S. and Ai.O.; methodology, T.S. and A.S.; software, T.S.; validation, A.S.; formal analysis, Ai.O.; investigation, T.S; resources, Ai.O. and As.O.; data curation, T.S.; writing-original draft preparation, T.S.; writing-review and editing, T.S. and Ai.O.; visualization, T.S.; supervision, Ai.O.; project administration, As.O.; funding acquisition, Ai.O.

Conflicts of Interest

The authors declare no conflict of interest.

References

1. Armato SG 3rd, McLennan G, Bidaut L, et al. The Lung Image Database Consortium (LIDC) and Image Database Resource Initiative (IDRI): a completed reference database of lung nodules on CT scans. *Med Phys*. 2011;38(2):915-931. doi:10.1118/1.3528204

2. Wu Y, Xia S, Liang Z, Chen R, Qi S. Artificial intelligence in COPD CT images: identification, staging, and quantitation. *Respir Res*. 2024;25(1):319. Published 2024 Aug 22. doi:10.1186/s12931-024-02913-z.

3. Esteva A, Robicquet A, Ramsundar B, et al. A guide to deep learning in healthcare. *Nat Med*. 2019;25(1):24-29. doi:10.1038/s41591-018-0316-z

4. Humphries SM, Notary AM, Centeno JP, et al. Deep Learning Enables Automatic Classification of Emphysema Pattern at CT. *Radiology*. 2020;294(2):434-444. doi:10.1148/radiol.2019191022

5. Fuhrman J, Yip R, Zhu Y, et al. Evaluation of emphysema on thoracic low-dose CTs through attention-based multiple instance deep learning. *Sci Rep*. 2023;13(1):1187. Published 2023 Jan 21. doi:10.1038/s41598-023-27549-9.

6. [Çallı E, Murphy K, Scholten ET, Schalekamp S, van Ginneken B. Explainable emphysema detection on chest radiographs with deep learning. *PLoS One*. 2022;17(7):e0267539. Published 2022 Jul 28. doi:10.1371/journal.pone.0267539

7. Almeida SD, Norajitra T, Lüth CT, et al. Prediction of disease severity in COPD: a deep learning approach for anomaly-based quantitative assessment of chest CT. *Eur Radiol*. 2024;34(7):4379-4392. doi:10.1007/s00330-023-10540-3.

8. Ash SY, Choi B, Oh A, Lynch DA, Humphries SM. Deep Learning Assessment of Progression of Emphysema and Fibrotic Interstitial Lung Abnormality. *Am J Respir Crit Care Med*. 2023;208(6):666-675. doi:10.1164/rccm.202211-2098OC

9. A. Wysoczanski, R. A. Hill, L. Yu, and K. Chen, "Robust deep labeling of radiological emphysema subtypes using squeeze and excitation CNNs," *arXiv preprint*, arXiv:2403.00257, Mar. 2024. [Online]. Available: https://arxiv.org/pdf/2403.00257

10. Tina Dorosti, Manuel Schultheiss, Felix Hofmann, Johannes Thalhammer, Luisa Kirchner, Theresa Urban, Franz Pfeiffer, Florian Schaff, Tobias Lasser, Daniela Pfeiffer, "Optimizing Convolutional Neural Networks for Chronic Obstructive Pulmonary Disease Detection in Clinical Computed Tomography Imaging" *arXiv preprint*, arXiv:2303.07189, Mar. 2023. [Online]. Available: https://arxiv.org/abs/2303.07189 https://doi.org/10.48550/arXiv.2303.07189

11. Zhu, Z., Zhao, S., Li, J. et al. Development and application of a deep learning-based comprehensive early diagnostic model for chronic obstructive pulmonary disease. *Respir Res 25*, 167 (2024). https://doi.org/10.1186/s12931-024-02793-3.

12. Fangfei Wang, Sixiang Li, Yuanxu Gao, Shiyue Li. Computed tomography-based artificial intelligence in lung disease-Chronic obstructive pulmonary disease. MEDCOMM – *Future Medicine*, 2024, 3(1): 73 https://doi.org/10.1002/mef2.73

13. Yeom JA, Kim KU, Hwang M, et al. Emphysema Quantification Using Ultra-Low-Dose Chest CT: Efficacy of Deep Learning-Based Image Reconstruction. *Medicina (Kaunas)*. 2022;58(7):939. Published 2022 Jul 15. doi:10.3390/medicina58070939

14. Ferri F, Bouzerar R, Auquier M, Vial J, Renard C. Pulmonary emphysema quantification at low dose chest CT using Deep Learning image reconstruction. *Eur J Radiol*. 2022;152:110338. doi:10.1016/j.ejrad.2022.110338.

15. M. Tjoa and C. Guan, "A survey on explainable artificial intelligence (XAI): Toward medical XAI," *IEEE Access*, vol. 9, pp. 118920–118940, 2020, https://doi.org/10.48550/arXiv.1907.07374 .

16. Zhou, L., Meng, X., Huang, Y. et al. An interpretable deep learning workflow for discovering subvisual abnormalities in CT scans of COVID-19 inpatients and survivors. *Nat Mach Intell* 4, 494–503 (2022). https://doi.org/10.1038/s42256-022-00483-7 .

17. W. Xie, T. H. Tran, and Y. Tang, "Emphysema subtyping on thoracic CT using deep neural networks," *arXiv preprint*, arXiv:2309.02576, Sep. 2023. [Online]. Available: https://arxiv.org/abs/2309.02576 http://dx.doi.org/10.48550/arXiv.2309.02576

18. Sourlos, N., Pelgrim, G., Wisselink, H.J. et al. Effect of emphysema on AI software and human reader performance in lung nodule detection from low-dose chest CT. *Eur Radiol Exp 8*, 63 (2024). https://doi.org/10.1186/s41747-024-00459-9

19. Park KJ, Bergin CJ, Clausen JL. Quantitation of emphysema with three-dimensional CT densitometry: comparison with two-dimensional analysis, visual emphysema scores, and pulmonary function test results. *Radiology*. 1999;211(2):541-547. doi:10.1148/radiology.211.2.r99ma52541.

20. M. D. Lynch et al., "CT-based visual and quantitative assessment of emphysema: association with mortality in the COPDGene study," *Radiology*, vol. 284, no. 2, pp. 570–579, 2017, doi: 10.1148/radiol.2017161552.

21. P. Hofmanninger et al., "Automatic lung segmentation in routine imaging is primarily a data diversity problem, not a methodology problem," *Eur. Radiol. Exp*., vol. 4, no. 1, p. 50, 2020, doi: 10.1186/s41747-020-00173-2.

22. Ash SY, Choi B, Oh A, Lynch DA, Humphries SM. Deep Learning Assessment of Progression of Emphysema and Fibrotic Interstitial Lung Abnormality. *Am J Respir Crit Care Med*. 2023;208(6):666-675. doi:10.1164/rccm.202211-2098OC.

23. Tang LYW, Coxson HO, Lam S, Leipsic J, Tam RC, Sin DD. Towards large-scale case-finding: training and validation of residual networks for detection of chronic obstructive pulmonary disease using low-dose CT. *Lancet Digit Health*. 2020;2(5):e259-e267. doi:10.1016/S2589-7500(20)30064-9

24. Bhati D, Neha F, Amiruzzaman M. A survey on explainable AI techniques for visualizing deep learning models in medical imaging. *J Imaging*. 2024;10(10):239. https://doi.org/10.3390/jimaging10100239.

25. Farhat H, Sakr GE, Kilany R. Deep learning applications in pulmonary medical imaging: recent updates and insights on COVID-19. *Mach Vis Appl*. 2020;31(6):53. doi:10.1007/s00138-020-01101-5.)

26. Hildt E. What is the role of explainability in medical artificial intelligence? *Bioengineering* (Basel). 2025;12(4):375. https://doi.org/10.3390/bioengineering12040375.

27. Mohamed Hoesein FA, de Hoop B, Zanen P, et al. CT-quantified emphysema in male heavy smokers: association with lung function decline. *Thorax*. 2011;66(9):782-787. doi:10.1136/thx.2010.145995.

28. Wang X, Qiao Y, Cui Y, et al. An explainable artificial intelligence framework for risk prediction of COPD in smokers. *BMC Public Health*. 2023;23(1):2164. Published 2023 Nov 6. doi:10.1186/s12889-023-17011-w .

29. Freyer N, et al. The ethical requirement of explainability for AI DSS in healthcare. *BMC Med Ethics*. 2024;25:116. https://doi.org/10.1186/s12910-024-01103-2.

Information about Authors:

Talshyn Sarsembayeva, Senior Lecturer, PhD candidate (EP AI in Medicine) at the Department of Artificial Intelligence and Big Data, Al-Farabi Kazakh National University (Almaty, Kazakhstan, e-mail: talshyn.sagdatbek@kaznu.edu.kz). Her research interests include medical image analysis, explainable artificial intelligence, and machine learning for diagnostic applications. She focuses on the development of interpretable AI models for population-level screening using CT imaging.

Ainash Oshibayeva, Candidate of Medical Sciences, Professor at the Department of Preventive Medicine and serves as Vice Rector for Strategic Development and Science at Khoja Akhmet Yassawi International Kazakh-Turkish University (Turkistan, Kazakhstan, e-mail: ainash.oshibayeva@ayu.edu.kz). Her work bridges public health, medical diagnostics, and data-driven research. She is involved in translational AI projects aiming to enhance clinical and preventive healthcare.

Assem Shayakhmetova, PhD, Associate Professor of the Department of Artificial Intelligence and Big Data at Al-Farabi Kazakh National University (Almaty, Kazakhstan, e-mail: asemshayakhmetova07@gmail.com). Her research focuses on the development of intelligent management systems, as well as the application of data mining methods and business process modeling. She actively participates in international and domestic scientific events, is the author of a number of scientific publications.

Assel Ospan, Senior Lecturer at the Department of Artificial Intelligence and Big Data, Al-Farabi Kazakh National University (Almaty, Kazakhstan, e-mail: assel.ospan@kaznu.edu.kz). Her research focuses on the development of intelligent models, information extraction using machine learning methods, and knowledge base construction. She actively participates in national AI research initiatives and has authored several publications.

Submission received: 21 August, 2025.
Revised: 19 November, 2025.
Accepted: 19 November, 2025.